2014

Spectral-domain optical coherence tomography staging and autofluorescence imaging in achromatopsia

J. P. Greenberg

J. Sherman

S. A. Zweifel

R. W. Chen

T. Duncker

See next page for additional authors

Authors
J. P. Greenberg, J. Sherman, S. A. Zweifel, R. W. Chen, T. Duncker, S. Kohl, B. Baumann, B. Wissinger, L. A. Yannuzzi, and S. H. Tsang

HHS Public Access

Author manuscript

JAMA Ophthalmol. Author manuscript; available in PMC 2015 May 07.

Published in final edited form as:

JAMA Ophthalmol. 2014 April 1; 132(4): 437–445. doi:10.1001/jamaophthalmol.2013.7987.

Spectral-Domain Optical Coherence Tomography Staging and Autofluorescence Imaging in Achromatopsia

Jonathan P. Greenberg, MD, **Jerome Sherman, OD**, **Sandrine A. Zweifel, MD**, **Royce W. S. Chen, MD**, **Tobias Duncker, MD**, **Susanne Kohl, MSc, PhD**, **Britta Baumann**, **Bernd Wissinger, MSc, PhD**, **Lawrence A. Yannuzzi, MD**, and **Stephen H. Tsang, MD, PhD**

Department of Ophthalmology, Columbia University, New York, New York (Greenberg, Chen, Duncker, Tsang); Department of Clinical Sciences, State University of New York College of Optometry, New York, New York (Sherman); The Vitreous, Retina, Macula Consultants of New York, New York (Zweifel, Yannuzzi); The LuEsther T. Mertz Retinal Research Center, Manhattan Eye, Ear, and Throat Hospital, New York, New York (Zweifel, Yannuzzi); Molecular Genetics Laboratory, Institute for Ophthalmic Research, Centre for Ophthalmology, University of Tübingen, Tübingen, Germany (Kohl, Baumann, Wissinger); Bernard and Shirlee Brown Glaucoma Laboratory, Edward S. Harkness Eye Institute, New York-Presbyterian Hospital, New York, New York (Tsang); Department of Pathology and Cell Biology, Columbia University, New York, New York (Tsang)

Abstract

Importance—Evidence is mounting that achromatopsia is a progressive retinal degeneration, and treatments for this condition are on the horizon.

Objectives—To categorize achromatopsia into clinically identifiable stages using spectral-domain optical coherence tomography and to describe fundus autofluorescence imaging in this condition.

Design, Setting, and Participants—A prospective observational study was performed between 2010 and 2012 at the Edward S. Harkness Eye Institute, New York-Presbyterian

Corresponding Author: Stephen H. Tsang, MD, PhD, Department of Ophthalmology, Columbia University, 160 Fort Washington Ave, Room 513, New York, NY 10032 (sht2@columbia.edu).

Author Contributions: Drs Tsang and Greenberg had full access to all the data in the study and take responsibility for the integrity of the data and the accuracy of the data analysis.
Study concept and design: Greenberg, Yannuzzi, Tsang.
Acquisition of data: Greenberg, Zweifel, Duncker, Kohl, Baumann, Tsang.
Analysis and interpretation of data: Greenberg, Sherman, Chen, Kohl, Baumann, Wissinger, Tsang.
Drafting of the manuscript: Greenberg, Kohl, Baumann, Tsang.
Critical revision of the manuscript for important intellectual content: Sherman, Zweifel, Chen, Duncker, Kohl, Wissinger, Yannuzzi, Tsang.
Statistical analysis: Greenberg, Tsang.
Obtained funding: Wissinger, Yannuzzi, Tsang.
Administrative, technical, or material support: Sherman, Chen, Duncker, Kohl, Baumann.
Study supervision: Zweifel, Wissinger, Yannuzzi, Tsang.

Conflict of Interest Disclosures: None reported.

Additional Contributions: Janet R. Sparrow, PhD, Department of Ophthalmology, Columbia University, provided helpful comments, and R. Theodore Smith, MD, PhD, Department of Ophthalmology, Columbia University (currently, Department of Ophthalmology, New York University) shared equipment. Neither received compensation for their contributions.

Hospital. Participants included 17 patients (aged 10-62 years) with full-field electroretinography-confirmed achromatopsia.

Main outcomes and Measures—Spectral-domain optical coherence tomography features and staging system, fundus autofluorescence and near-infrared reflectance features and their correlation to optical coherence tomography, and genetic mutations served as the outcomes and measures.

Results—Achromatopsia was categorized into 5 stages on spectral-domain optical coherence tomography: stage 1 (2 patients [12%]), intact outer retina; stage 2 (2 patients [12%]), inner segment ellipsoid line disruption; stage 3 (5 patients [29%]), presence of an optically empty space; stage 4 (5 patients [29%]), optically empty space with partial retinal pigment epithelium disruption; and stage 5 (3 patients [18%]), complete retinal pigment epithelium disruption and/or loss of the outer nuclear layer. Stage 1 patients showed isolated hyperreflectivity of the external limiting membrane in the fovea, and the external limiting membrane was hyperreflective above each optically empty space. On near infrared reflectance imaging, the fovea was normal, hyporeflective, or showed both hyporeflective and hyperreflective features. All patients demonstrated autofluorescence abnormalities in the fovea and/or parafovea: 9 participants (53%) had reduced or absent autofluorescence surrounded by increased autofluorescence, 4 individuals (24%) showed only reduced or absent autofluorescence, 3 patients (18%) displayed only increased autofluorescence, and 1 individual (6%) exhibited decreased macular pigment contrast. Inner segment ellipsoid line loss generally correlated with the area of reduced autofluorescence, but hyperautofluorescence extended into this region in 2 patients (12%). Bilateral coloboma-like atrophic macular lesions were observed in 1 patient (6%). Five novel mutations were identified (4 in the *CNGA3* gene and 1 in the *CNGB3* gene).

Conclusions and Relevance—Achromatopsia often demonstrates hyperautofluorescence suggestive of progressive retinal degeneration. The proposed staging system facilitates classification of the disease into different phases of progression and may have therapeutic implications.

Achromatopsia is a congenital cone photoreceptor disorder with autosomal recessive inheritance and an estimated prevalence of 1 in 30 000. Affected individuals usually have congenital nystagmus, poor visual acuity, photophobia, and lack of color discrimination.[1] Funduscopic examination is often normal, although pigmentary mottling and atrophic changes may be observed in the macula.[2] Electroretinography (ERG) reveals absent or profoundly reduced cone responses with normal or mildly subnormal rod function.[3] These features establish the clinical diagnosis of achromatopsia. Causative mutations have been identified in the *CNGB3* (Chr. 8q21.3), *CNGA3* (Chr. 2q11.2), *GNAT2* (Chr.1p13.3), *PDE6C* (Chr. 10q23.33), and *PDE6H* (Chr. 12p12.3) genes, with CNGB3 being the most commonly affected.[4-9] All of these genes encode functionally important components of the cone photo-transduction cascade.

Achromatopsia has traditionally been thought of as a stationary disease and was classified as part of the cone dysfunction syndromes rather than the cone dystrophies.[1] However, findings in animal models and in human studies have suggested that achromatopsia is rather a progressive degeneration. Mouse models of achromatopsia have demonstrated a progressive

loss of the cone cells with age,[10,11] canine models have shown detectable cone ERG function in young pups that becomes nonrecordable in mature dogs,[12] and human studies[3] of achromatopsia have revealed deterioration in cone ERG function over time. Recently, studies[2,13] have used spectral-domain optical coherence tomography(SD-OCT) to show age-dependent correlations with reduced outer nuclear layer (ONL) and total retinal thicknesses, disruption of the inner segment ellipsoid (ISe) line, the presence of an optically empty space (OES) (also called a *bubble* or *hyporeflective zone*) in the cone photoreceptor layers, and retinal pigment epithelium (RPE) disruption. Most recently, a longitudinal study[14] evidenced progressive structural degeneration in children younger than 10 years with achromatopsia. Over a mean follow-up period of 16 months, these individuals showed a decrease in central macular and ONL thicknesses as well as new or enlarging disruption of the ISe line.

Treatments for achromatopsia are on the horizon. Cone-targeted gene therapy has shown success in mouse and canine studies,[15-17] in which it improved cone survival, recovered cone ERG amplitudes to near-normal levels, and corrected visual acuity. Another promising treatment is the use of neuroprotective compounds, most notably ciliary neurotrophic factor (CNTF), which has been shown[18] to inhibit progressive degeneration of rod and cone photoreceptors in a variety of animal models and clinical trials. It also induced cone outer-segment regeneration in a rat model of retinal degeneration[19] and improved cone ERG function and vision in dogs with achromatopsia.[18] Therefore, long-term treatment with CNTF starting at early stages of degeneration could be a viable strategy for preservation and rescue of cone photoreceptors. However, success with either gene- or CNTF-based therapy would require that cone photoreceptors are present and viable within the macula. Although there are still many hurdles to overcome, stem cell–based therapy is being pursued as a potential treatment of retinal degenerative diseases and may become an option for patients who have already lost their foveal cones. However, if RPE atrophy is also present, replacement of the RPE would be an additional consideration and may result in more challenging treatment.[20,21] Therefore, a system of clinically distinguishable stages may facilitate better classification of the disease at different phases of its progression and guide therapeutic decisions, not only in clinical trials but in clinical settings as well. In the present study, we propose such a system, which is based on SD-OCT because it provides high-resolution imaging of retinal architecture and is widely available and easy to perform.

Another imaging modality, which is widely used in the diagnosis, characterization, and follow-up of many retinal disorders, is fundus autofluorescence (AF). This technique enables visualization of the distribution of lipofuscin across the posterior pole. Lipofuscin contains a complex mixture of fluorescent molecules that are by-products of the visual cycle and are accumulated in the RPE through phagocytosis of photo-receptor outer segments.[22] Although the diffuse increase of lipofuscin with aging is physiologic,[23] abnormal distributions are common in many retinal diseases and result in topographic changes in intensity on AF images.[24-27] Decreased AF is typically considered to be a marker of RPE atrophy, but it may also indicate photoreceptor loss (arrested bisretinoid deposition) combined with photodegradation of RPE lipofuscin.[28] On the other hand, elevated AF suggests an increased metabolic load at an intermediate stage before cell loss and

atrophy.[22,26] For example, adenosine triphosphate binding cassette A4 (ABCA4)–related disease and cone-rod dystrophies of other origins can present with hyperautofluorescent rings that surround decreased or absent foveal AF and progressively expand with time.[26,29] These rings colocalize with reduced visual sensitivity[27] and, across the annulus, the ISe line may not be visible on SD-OCT.[30] Given the mounting evidence for the progressive nature of achromatopsia, one may expect to observe AF features similar to those seen in other progressive degenerations. We describe these features and compare them with structural changes as observed on SD-OCT.

Methods

Seventeen patients (11 [65%] males, 6 [35%] females; mean [SD] age, 31 [16] years; range, 10-62 years) with achromatopsia were included in this study. There were 4 sibling pairs. The study was performed between February 2010 and May 2012 at the Edward S. Harkness Eye Institute. The research adhered to the tenets of the Declaration of Helsinki, institutional review board approval was granted, written informed consent was obtained from participants or parents/guardians, and Health Insurance Portability and Accountability Act compliance was maintained. Participants received no monetary compensation. Experienced electrophysiologists performed full-field ERGs according to the International Society for Clinical Electrophysiology of Vision standards.[31] The diagnosis was based on clinical presentation of poor visual acuity since birth, congenital nystagmus, photophobia, severe color vision defects, and absent or residual cone responses with normal rod responses on ERG. Participants were screened in a step-by-step strategy for mutations in the *CNGB3* (OMIM 605080), *CNGA3* (OMIM 600053), *GNAT2* (OMIM 139340), *PDE6C* (OMIM 600827), and *PDE6H* (OMIM 601190) genes, as previously described.[5,6]

All patients underwent a detailed ophthalmic examination; imaging included color fundus photography as well as near-infrared reflectance (NIR), AF, and SD-OCT imaging performed with a confocal scanning laser ophthalmoscope (Spectralis HRA+OCT, Heidelberg Engineering). Autofluorescence images (488 nm excitation, 500-680 nm barrier filter) were composed of at least 9 single frames (30° × 30° field, highspeed setting), which were computationally averaged to improve signal to noise ratio. However, fewer frames were used in some cases when image acquisition was difficult. Spectralis OCTs were performed as single horizontal line scans across the foveal center. The high-resolution setting was used, and 40to 100 frames per scan were obtained; however, these were adjusted when severe nystagmus and poor fixation impaired OCT tracking. Each SD-OCT scan was correlated in real time with either an NIR (NIR-OCT) or AF (AF-OCT) image (Eye Explorer software; Heidelberg Engineering). The NIR-OCT images were obtained for all participants; however, AF-OCT imaging was possible only with 6 individuals (35%) because of difficult image acquisition. For the remaining 11 cases (65%), aligning AF to NIR images with software written in MATLAB, version 7.10 (http://www.mathworks.com/products/matlab/) enabled accurate correlation between AF and SD-OCT.

Results

Clinical characteristics of the patients are summarized in Table 1. All participants had photophobia and congenital nystagmus. Snellen best-corrected visual acuity ranged from 20/80 to 20/200 (mean, 20/150) and was generally symmetrical.

Participants demonstrated largely symmetrical findings on all imaging modalities. On color fundus photography, 7 patients (41%) showed RPE alterations: 3 of these (18%) were mottled RPE changes and 4 (23%) were a distinct area of RPE atrophy. Another patient had bilateral coloboma-like atrophic macular lesions, with excavation down to the sclera (further detail is available in the Supplement [eAppendix 1]). Of the patients with no visible RPE changes, 2 had a darkened fovea (12%), 2 showed a hypopigmented foveola (12%), and in 5 cases, the fovea appeared normal (29%). On NIR imaging, 9 patients (53%) had a hyporeflective fovea, with a distinct central zone of hyperreflectance in 3 of these cases (18%). The fovea in 5 patients (29%) showed mixed hyporeflective and hyperreflective features, and in 3 individuals (18%) appeared normal.

Autofluorescence imaging was more sensitive for detecting pathologic features than both color fundus photography and NIR imaging and demonstrated abnormalities in all patients. An area of reduced AF was observed in the central macula of 13 participants (76%). It was often in the shape of a horizontal oval and was limited to the fovea, although 2 patients (12%) had larger lesions extending into the parafovea. In 8 cases (47%), a region of hyperautofluorescence surrounded the reduced AF, and 1case (6%) showed bordering hyperautofluorescence limited to the inferior and temporal para-fovea. Of the 4 patients (24%) without reduced AF, 3 individuals (18%) demonstrated hyperautofluorescence and 1 patient (6%) showed decreased macular pigment contrast. The area of hyperautofluorescence was generally greater in horizontal than vertical extent and ranged in width from a thin rim surrounding reduced AF to a wider region that extended into the para-fovea.

On SD-OCT, 13 participants (76%) had foveal hypoplasia.[32] The ISe line was disrupted in 15 patients (88%), and 8 of these (47%)showed varying degrees of RPE disruption. Achromatopsia was categorized based on SD-OCT into 5 stages (Figure 1; retinal layer nomenclature is listed in the Supplement [eFigure]). Stage 1 disease (2 patients [12%]) was characterized by intact outer retinal structure, although subtle discontinuities were observed in the ISe line. The cone outer segment tip layer appeared normal in 1 of these patients (6%) and was present but thinned toward the foveal center in the other patient (6%). We also observed isolated hyperreflectivity of the external limiting membrane (ELM) in the fovea and flattening of the ISe line posterior to the foveola. Stage 2 disease (2 patients [12%]) was defined as disruption of the ISe line but without the presence of an OES. The photoreceptor inner segment layer was present in these patients, although it was hyperreflective in 1 patient (6%) above and slightly beyond the site of ISe line disruption, where it likely represented a transitional phase toward inner segment breakdown. We observed interruption of the cone outer segment tip layer in 1 of these patients (6%), but image quality in the other individual (6%) was insufficient to differentiate this feature. Stage 3 disease (5 patients [29%]) demonstrated an OES with loss of photoreceptor inner and outer segments, but there was no

visible RPE damage. In most cases, we observed extension of the OES into the ONL. Stage 4 disease (5 patients [29%]) was defined as the presence of an OES with partial RPE disruption. The ELM above each OES was hyperreflective, and it was thickened in 3 of these cases. Stage 5 disease (3 patients [18%]) was defined as complete RPE disruption and/or loss of the ONL. One of these cases (6%) had complete RPE disruption and loss of the OES, 1 had both complete RPE disruption and ONL loss (6%), and the third patient (6%) had bilateral coloboma-like macular lesions. There was no significant difference in age between SD-OCT stages of disease (1-way analysis of variance $F = 0.78$; $P = .56$), although both patients with stage 1 achromatopsia were younger than 24 years, and stage did not correlate with visual acuity or with which gene was affected by mutation (*CNGB3* vs *CNGA3*), which is in line with the lack of geno-type-phenotype correlations previously described.[2,33] There was some degree of phenotypic concordance between sibling pairs, with siblings in 2 of the 4 pairs displaying the same phenotype on all imaging modalities (pairs 2 and 3; both stage 4). Although both of the oldest siblings (pair 4) had stage 5 disease and displayed the largest lesions of the study group, only one demonstrated bilateral coloboma-like macular lesions. In sibling pair 1, the brother had stage 3 disease, but the sister, of similar age, had stage 1. More detail is available in the Supplement (eAppendix 2).

Various comparisons were made between imaging modalities (Figure 2). The region of ISe loss generally corresponded to the area of reduced AF, although hyperautofluorescence extended into this region in 2 patients (12%). Near-infrared reflectance imaging usually displayed an area of hyporeflectance that correlated with the region of ISe line disruption. Patients with an intact outer retinal structure did not have reduced foveal AF and appeared normal on funduscopy and NIR imaging. Spectral-domain OCT evidenced RPE disruption in all cases in which RPE changes were visible on funduscopy, and these patients showed corresponding hyperreflective features on NIR imaging and greatly reduced or absent AF. No other imaging modality in this study reliably differentiated between all SD-OCT stages.

Genetic analysis revealed causative homozygous or compound heterozygous mutations in *CNGA3* for 7 participants (41%) and in *CNGB3* for 3 people (18%); single heterozygous mutations in *CNGB3* were identified in 2 participants (12%). Five mutations (29%) were novel (4 [24%] in *CNGA3* and 1 [6%] in *CNGB3*). No mutations were detected in *GNAT2*, *PDE6C*, or *PDE6H*. The observed genotypes are documented in Table 2 (further detail is available in the Supplement [eAppendix 3]).

Discussion

One objective of our study was to evaluate the AF features of achromatopsia. Being a primary cone photoreceptor disorder, the area of hyperautofluorescence found in most (12 [71%]) of our patients likely reflects increased cone outer segment turnover, which is marked by intensified bisretinoid deposition in the RPE. Low calcium levels in *CNGA3*- and *CNGB3*-deficient cones may affect endoplasmic reticulum metabolism and outer segment biogenesis. Given the evidence from previous studies[2,3,13,14] that achromatopsia is a progressive disorder, our finding of hyperautofluorescence is not surprising. However, the observed hyperautofluorescence was often subtle and, in 3 patients (18%) with early-stage disease, was visible only on one side of the fovea. For the cases without

hyperautofluorescence, the slow rate of photoreceptor damage in combination with masking of the AF signal by macular pigment may have resulted in the AF images not manifesting the abnormalities in outer segment turnover. Green light AF, which excludes macular pigment, and estimation of macular pigment density could be helpful for a more precise degree of autofluorescence derived from RPE lipofuscin in the macula. This assessment may be further aided by AF quantification.[34]

Patients with RPE disruption demonstrated on SD-OCT displayed a corresponding area of greatly reduced or absent AF. However, 5 (29%) of the 7 individuals (41%) who had ISe line disruption but no RPE damage also showed reduced AF (less marked than in those with RPE atrophy), which was localized to regions of photoreceptor loss. This suggests that the reduced AF in these patients arises from arrested deposition of bisretinoids in the RPE (due to the absence of photoreceptors) coupled with lipofuscin depletion due to photodegradation.[28] The area of hyperautofluorescence was generally observed in regions where the ISe line was present, indicating that it preceded photoreceptor loss. However, in 2 patients (12%; both with stage 3 achromatopsia) it extended into the region of ISe loss, likely reflecting areas where photodegradation had not yet substantially reduced AF intensity. Longitudinal data in future studies would be helpful to evidence changes in AF intensity over time and correlate them with features observed on SD-OCT.

We believed SD-OCT to be the optimal modality with which to stage achromatopsia because it provides high-resolution imaging of retinal architecture and is widely available and easy to perform. In contrast, other techniques, such as adaptive optics and multifocal ERG, are difficult to perform in achromatopsia because of the nystagmus and poor fixation inherent to this condition. These techniques are therefore not practical for a clinically accessible staging system, but may be useful adjunctive measures for tracking structural and functional responses to treatment in clinical trials. Our system relies on SD-OCT alone for simplicity but also because no other imaging modality in our study reliably differentiated between all stages. It is primarily based on the integrity of cone photoreceptors, but also takes into account damage to the RPE. The degree of structural degeneration categorized by this staging system may guide selection of optimal treatment strategies not only for clinical trials, but in clinical settings as well. Although our study was limited by its cross-sectional design and fairly small sample size, our assessment of the clinical course of achromatopsia was guided by the age-dependent correlations demonstrated in previous cross-sectional SD-OCT studies[2,13] and by the dynamic retinal changes evidenced in a recent longitudinal study.[14]

Patients with stage 1 achromatopsia had an intact outer retinal structure, with only subtle discontinuities in the ISe line and a relatively preserved cone outer segment tip layer in the fovea. This indicates that the cone photoreceptors maintained structural integrity; these patients would therefore be ideal candidates for gene therapy. They would also be most likely to benefit from treatment with CNTF, which may arrest cone degeneration and possibly also recover their function, as it did in dogs with *CNGB3* mutations.[18] An interesting feature that we observed in these cases was increased reflectivity of the foveal ELM. This was observed in the absence of hyperreflective foveal cone outer segments, which was shown to be a transitional phase toward ISe line disruption,[14] and thus the ELM

appears to be the first structure to demonstrate hyper-reflectance. Although this feature was subtle in one patient, it was more prominent and extended over a larger region in the other patient, where it corresponded to the region of cone outer segment tip thinning. The observed ELM hyperreflectivity may be explained by a greater difference in refractive index as tissue below it breaks down, for which it appears to be a sensitive indicator. Therefore, isolated hyperreflectivity of the ELM may represent an early sign of cone degeneration detectable on SD-OCT.

Stage 2 was defined by disruption of the ISe line. Although these patients had loss of the photoreceptor outer segments, the photoreceptor inner segment layer was relatively spared. Gene therapy has not been shown to regenerate cone cells, but long-term treatment with CNTF induced cone outer segment regeneration in a rat model of retinal degeneration.[19] Therefore, there may be potential for CNTF to not only arrest the degenerative process but also to regenerate the focal cone damage in these patients.

Photoreceptor damage was more extensive in patients with stage 3 and 4 disease, who showed loss of both the photoreceptor inner and outer segments in the OES. It is suspected that many cone nuclei are ectopically located in these patients (Supplement [eAppendix 4]). However, the ONL was still present, which suggests that these patients retain some viable and correctly located nuclei. They may therefore experience some success with treatments aimed at photoreceptor regeneration, although photoreceptor replacement with stem cell therapy may be the most suitable treatment. Of note are 2 reported[13,14] cases of patients who presented with an OES beneath an only intermittently disrupted ISe line (Supplement [eAppendix 5]).

Patients with stage 4 achromatopsia demonstrated partial RPE disruption within the region of the OES. Previous studies[2,33] found RPE atrophy only in olderage groups, and we observed several patients with an OES but with no signs of RPE disruption. This suggests that RPE disruption is a late manifestation in achromatopsia. The secondary RPE damage may be explained, at least in part, by the toxic effects of lipofuscin accumulation in these cells.[35-37] When considering an optimal treatment protocol for patients with RPE disruption, regeneration or replacement of the RPE would be an additional consideration and may result in more challenging treatment.[20,21] Ciliary neurotrophic factor has been shown[38] to increase RPE survival in cultures of human fetal RPE cells and therefore may have the additional benefit of preventing or stabilizing RPE damage in patients with achromatopsia.

In stage 5 disease, there was complete RPE disruption and/or loss of the ONL. Other studies[2,33] have illustrated similar cases of achromatopsia. Given that foveal photoreceptors and/or RPE cells are not viable in these patients, they would require replacement with stem cell therapy. However, the case with bilateral coloboma-like atrophic macular lesions would require more extensive regenerative approaches.

Although animal models have shown promising results, knowledge regarding the extent of regeneration with different treatment approaches is still in the early stages, and much work needs to be done to determine how humans with achromatopsia will respond to the proposed therapies. Although this staging system is based on which treatments may restore the outer

retina, to successfully restore vision, the inner retinal cells and central visual pathways will need to usefully process the new peripheral input from functional cones. Success in this regard may be age dependent, with one study[17] showing that older dogs were less likely than younger dogs to show restoration of cone ERG responses after gene therapy, even though many cones were present and structurally normal, and another study[16] demonstrating that gene therapy recovered ERG amplitudes in older mice but without a corresponding improvement in visual acuity.

Limitations of the study include its relatively small sample size, which provided few patients in each SD-OCT stage. A larger study may afford more consistent correlations of the stages with the progressive features of multimodal imaging as well as with age and visual acuity. This study was also limited by the lack of confirmed disease-causing mutations in 7 patients; total genome sequencing may aid in elucidating genotype-phenotype relationships. Given the cross-sectional design of this study, longitudinal data may provide a better understanding of the pathophysiology of achromatopsia and may contribute further evidence of its progressive nature.

Conclusions

Achromatopsia often exhibits AF features that suggest progressive retinal degeneration. Autofluorescence imaging provides a modality to topographically visualize the pathologic changes and reveals features that are not otherwise appreciated; it may therefore provide some additional clinical usefulness, as suggested by the observations in this report. The foveal ELM appears to be the first structure to develop hyper-reflectivity and may be an early sign of cone degeneration in patients with intact outer retina. The proposed SD-OCT staging system may be used to guide therapeutic decisions.

Supplementary Material

Refer to Web version on PubMed Central for supplementary material.

Acknowledgments

Funding/Support: This study was supported, in part, by grants EY018213 (Dr Tsang) and RO1-EY02115 (R. Theodore Smith) from the National Eye Institute/National Institutes of Health; P30EY019007 from Core Support for Vision Research, Columbia University; C026448 from New York Stem Cell Science; Foundation Fighting Blindness; the Macula Foundation Inc; TS080017 from the Department of Defense; and unrestricted funds from Research to Prevent Blindness. Dr Tsang is a Burroughs-Wellcome Program in Biomedical Sciences Fellow, and is also supported by the Charles E. Culpeper–Partnership for Cures 07-CS3, Crowley Research Fund, Schneeweiss Stem Cell Fund, New York State grant N09G-302, and a Joel Hoffmann Scholarship.

Role of the Sponsor: None of the sponsors or funding organizations had a role in the design and conduct of the study; collection, management, analysis, and interpretation of the data; preparation, review, or approval of the manuscript; and decision to submit the manuscript for publication.

References

1. Michaelides M, Hunt DM, Moore AT. The cone dysfunction syndromes. Br J Ophthalmol. 2004; 88(2):291–297. [PubMed: 14736794]

2. Thiadens AA, Somervuo V, van den Born LI, et al. Progressive loss of cones in achromatopsia: an imaging study using spectral-domain optical coherence tomography. Invest Ophthalmol Vis Sci. 2010; 51(11):5952–5957. [PubMed: 20574029]

3. Khan NW, Wissinger B, Kohl S, Sieving PA. CNGB3 achromatopsia with progressive loss of residual cone function and impaired rod-mediated function. Invest Ophthalmol Vis Sci. 2007; 48(8): 3864–3871. [PubMed: 17652762]

4. Kohl S, Marx T, Giddings I, et al. Total colourblindness is caused by mutations in the gene encoding the alpha-subunit of the cone photoreceptor cGMP-gated cation channel. Nat Genet. 1998; 19(3):257–259. [PubMed: 9662398]

5. Kohl S, Baumann B, Broghammer M, et al. Mutations in the CNGB3 gene encoding the beta-subunit of the cone photoreceptor cGMP-gated channel are responsible for achromatopsia (ACHM3) linked to chromosome 8q21. Hum Mol Genet. 2000; 9(14):2107–2116. [PubMed: 10958649]

6. Kohl S, Baumann B, Rosenberg T, et al. Mutations in the cone photoreceptor G-protein alpha-subunit gene GNAT2 in patients with achromatopsia. Am J Hum Genet. 2002; 71(2):422–425. [PubMed: 12077706]

7. Thiadens AA, den Hollander AI, Roosing S, et al. Homozygosity mapping reveals PDE6C mutations in patients with early-onset cone photoreceptor disorders. Am J Hum Genet. 2009; 85(2): 240–247. [PubMed: 19615668]

8. Kohl S, Coppieters F, Meire F, et al. European Retinal Disease Consortium. A nonsense mutation in PDE6H causes autosomal-recessive incomplete achromatopsia. Am J Hum Genet. 2012; 91(3):527–532. [PubMed: 22901948]

9. Thiadens AA, Slingerland NW, Roosing S, et al. Genetic etiology and clinical consequences of complete and incomplete achromatopsia. Ophthalmology. 2009; 116(10):1984–1989.e1.10.1016/j.ophtha.2009.03.053 [PubMed: 19592100]

10. Biel M, Seeliger M, Pfeifer A, et al. Selective loss of cone function in mice lacking the cyclic nucleotide-gated channel CNG3. Proc Natl Acad Sci U S A. 1999; 96(13):7553–7557. [PubMed: 10377453]

11. Ding XQ, Harry CS, Umino Y, Matveev AV, Fliesler SJ, Barlow RB. Impaired cone function and cone degeneration resulting from CNGB3 deficiency: down-regulation of CNGA3 biosynthesis as a potential mechanism. Hum Mol Genet. 2009; 18(24):4770–4780. [PubMed: 19767295]

12. Sidjanin DJ, Lowe JK, McElwee JL, et al. Canine CNGB3 mutations establish cone degeneration as orthologous to the human achromatopsia locus ACHM3. Hum Mol Genet. 2002; 11(16):1823–1833. [PubMed: 12140185]

13. Thomas MG, Kumar A, Kohl S, Proudlock FA, Gottlob I. High-resolution in vivo imaging in achromatopsia. Ophthalmology. 2011; 118(5):882–887. [PubMed: 21211844]

14. Thomas MG, McLean RJ, Kohl S, Sheth V, Gottlob I. Early signs of longitudinal progressive cone photoreceptor degeneration in achromatopsia. Br J Ophthalmol. 2012; 96(9):1232–1236. [PubMed: 22790432]

15. Michalakis S, Mühlfriedel R, Tanimoto N, et al. Restoration of cone vision in the CNGA3$^{-/-}$ mouse model of congenital complete lack of cone photoreceptor function. Mol Ther. 2010; 18(12):2057–2063. [PubMed: 20628362]

16. Carvalho LS, Xu J, Pearson RA, et al. Long-term and age-dependent restoration of visual function in a mouse model of CNGB3-associated achromatopsia following gene therapy. Hum Mol Genet. 2011; 20(16):3161–3175. [PubMed: 21576125]

17. Komáromy AM, Alexander JJ, Rowlan JS, et al. Gene therapy rescues cone function in congenital achromatopsia. Hum Mol Genet. 2010; 19(13):2581–2593. [PubMed: 20378608]

18. Wen R, Tao W, Li Y, Sieving PA. CNTF and retina. Prog Retin Eye Res. 2012; 31(2):136–151. [PubMed: 22182585]

19. Li Y, Tao W, Luo L, et al. CNTF induces regeneration of cone outer segments in a rat model of retinal degeneration. PLoS One. 2010; 5(3):e9495.10.1371/journal.pone.0009495 [PubMed: 20209167]

20. Dahlmann-Noor A, Vijay S, Jayaram H, Limb A, Khaw PT. Current approaches and future prospects for stem cell rescue and regeneration of the retina and optic nerve. Can J Ophthalmol. 2010; 45(4):333–341. [PubMed: 20648090]
21. Huang Y, Enzmann V, Ildstad ST. Stem cell–based therapeutic applications in retinal degenerative diseases. Stem Cell Rev. 2011; 7(2):434–445. [PubMed: 20859770]
22. Sparrow JR, Yoon KD, Wu Y, Yamamoto K. Interpretations of fundus autofluorescence from studies of the bisretinoids of the retina. Invest Ophthalmol Vis Sci. 2010; 51(9):4351–4357. [PubMed: 20805567]
23. Delori FC, Goger DG, Dorey CK. Age-related accumulation and spatial distribution of lipofuscin in RPE of normal subjects. Invest Ophthalmol Vis Sci. 2001; 42(8):1855–1866. [PubMed: 11431454]
24. Boon CJ, Jeroen Klevering B, Keunen JE, Hoyng CB, Theelen T. Fundus autofluorescence imaging of retinal dystrophies. Vision Res. 2008; 48(26):2569–2577. [PubMed: 18289629]
25. Holz FG, Bellman C, Staudt S, Schütt F, Völcker HE. Fundus autofluorescence and development of geographic atrophy in age-related macular degeneration. Invest Ophthalmol Vis Sci. 2001; 42(5):1051–1056. [PubMed: 11274085]
26. Robson AG, Michaelides M, Luong VA, et al. Functional correlates of fundus autofluorescence abnormalities in patients with RPGR or RIMS1 mutations causing cone or cone rod dystrophy. Br J Ophthalmol. 2008; 92(1):95–102. [PubMed: 17962389]
27. Robson AG, Michaelides M, Saihan Z, et al. Functional characteristics of patients with retinal dystrophy that manifest abnormal parafoveal annuli of high density fundus autofluorescence; a review and update. Doc Ophthalmol. 2008; 116(2):79–89. [PubMed: 17985165]
28. Sparrow JR, Gregory-Roberts E, Yamamoto K, et al. The bisretinoids of retinal pigment epithelium. Prog Retin Eye Res. 2012; 31(2):121–135. [PubMed: 22209824]
29. Michaelides, M. Fundus autofluorescence in cone and cone-rod dystrophies. In: Lois, N.; Forrester, JV., editors. Fundus Autofluorescence. Philadelphia, PA: Lippincott Williams & Wilkins; 2009. p. 153-166.
30. Gomes NL, Greenstein VC, Carlson JN, et al. A comparison of fundus autofluorescence and retinal structure in patients with Stargardt disease. Invest Ophthalmol Vis Sci. 2009; 50(8):3953–3959. [PubMed: 19324865]
31. Marmor MF, Fulton AB, Holder GE, Miyake Y, Brigell M, Bach M. International Society for Clinical Electrophysiology of Vision. ISCEV Standard for full-field clinical electroretinography (2008 update). Doc Ophthalmol. 2009; 118(1):69–77. [PubMed: 19030905]
32. McAllister JT, Dubis AM, Tait DM, et al. Arrested development: high-resolution imaging of foveal morphology in albinism. Vision Res. 2010; 50(8):810–817. [PubMed: 20149815]
33. Genead MA, Fishman GA, Rha J, et al. Photoreceptor structure and function in patients with congenital achromatopsia. Invest Ophthalmol Vis Sci. 2011; 52(10):7298–7308. [PubMed: 21778272]
34. Delori F, Greenberg JP, Woods RL, et al. Quantitative measurements of autofluorescence with the scanning laser ophthalmoscope. Invest Ophthalmol Vis Sci. 2011; 52(13):9379–9390. [PubMed: 22016060]
35. Holz FG, Schütt F, Kopitz J, et al. Inhibition of lysosomal degradative functions in RPE cells by a retinoid component of lipofuscin. Invest Ophthalmol Vis Sci. 1999; 40(3):737–743. [PubMed: 10067978]
36. Sparrow JR, Cai B, Jang YP, Zhou J, Nakanishi K. A2E, a fluorophore of RPE lipofuscin, can destabilize membrane. Adv Exp Med Biol. 2006; 572:63–68. [PubMed: 17249556]
37. Sparrow JR, Nakanishi K, Parish CA. The lipofuscin fluorophore A2E mediates blue light–induced damage to retinal pigmented epithelial cells. Invest Ophthalmol Vis Sci. 2000; 41(7):1981–1989. [PubMed: 10845625]
38. Li R, Wen R, Banzon T, Maminishkis A, Miller SS. CNTF mediates neurotrophic factor secretion and fluid absorption in human retinal pigment epithelium. PLoS One. 2011; 6(9):e23148.10.1371/journal.pone.0023148 [PubMed: 21912637]

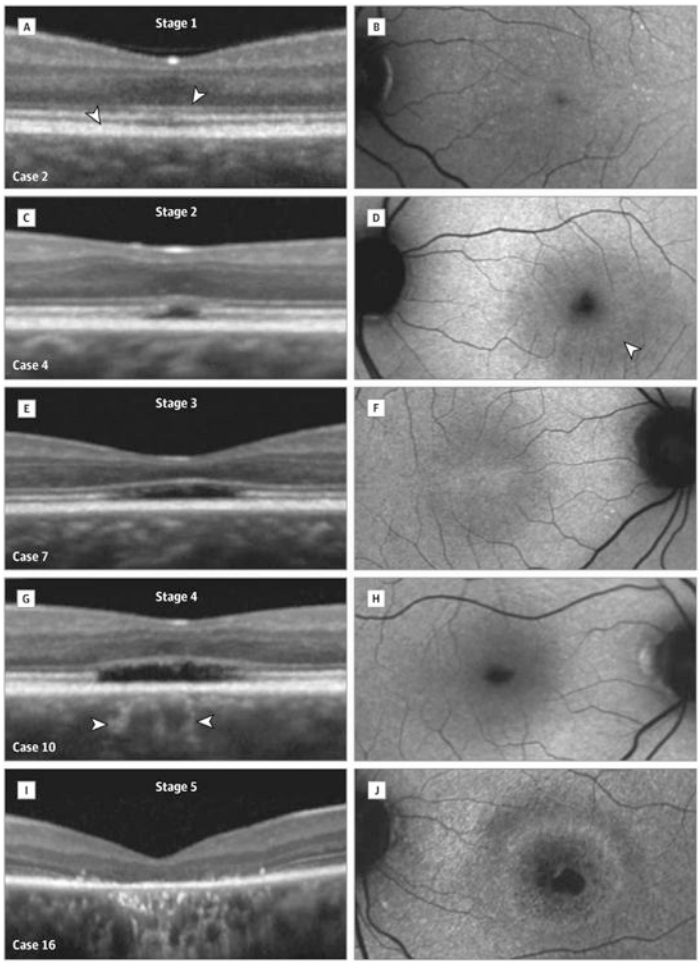

Figure 1. Staging System and Corresponding Fundus Autofluorescence (AF) Images

Spectral-domain optical coherence tomography (SD-OCT) stages (left) and corresponding fundus AF images (right) in patients with achromatopsia. Stage 1: A, Outer retinal structure is intact but there is flattening and subtle discontinuity of the inner segment ellipsoid (ISe) line posterior to the foveola. The cone outer segment tip (COST) layer (left arrowhead) is relatively spared, although it is thinned toward the foveal center, and the external limiting membrane is hyperreflective (right arrowhead) in this region. B, The corresponding AF image shows decreased macular pigment contrast and fine punctate hyperautofluorescent dots scattered across the macula (the dots were also visible on color fundus photography [yellow] and near-infrared reflectance imaging [hyperreflective]). Stage 2: C, The ISe line is disrupted. Note interruption of the COST layer and hyperreflectivity of the photoreceptor inner segments. D, The AF image shows centrally reduced AF with subtle hyperautofluorescence around the inferotemporal fovea (arrowhead). Stage 3: E, This case demonstrates the classic optically empty space (OES), with absent photoreceptors in the fovea, but the retinal pigment epithelium (RPE) appears intact. F, The AF image shows hyperautofluorescence resulting in a stippled foveal appearance. Stage 4: G, An OES and partial RPE disruption (choroidal hyperreflectance is indicated with arrowheads). Note the reflective material, possibly photoreceptor debris, at the roof of the OES (also seen in E). H, The AF image displays a central area of greatly reduced AF but no observable

hyperautofluorescence. Stage 5: I, Complete RPE disruption and loss of the outer nuclear layer. J, The AF image demonstrates a larger lesion with a surrounding hyperautofluorescent ring and a central region of absent AF.

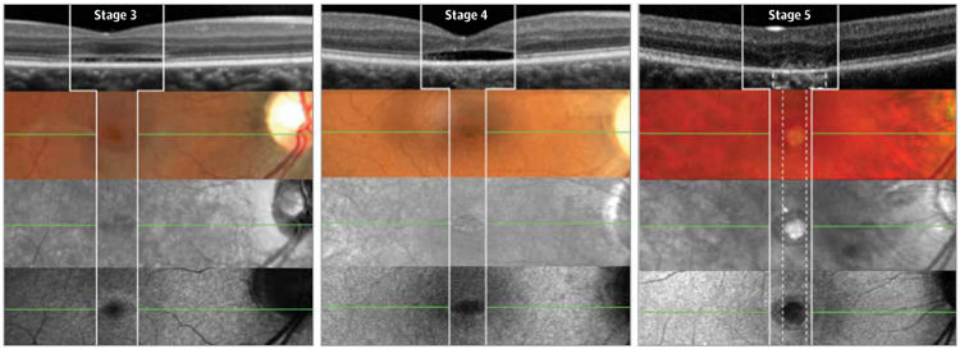

Figure 2. Multimodal Imaging

Images in patients with stage 3 (case 5), stage 4 (case 12), and stage 5 (case 15) achromatopsia are shown. Imaging modalities (top to bottom) are spectral-domain optical coherence tomography (SD-OCT), color fundus photography (color), near-infrared reflectance (NIR), and fundus autofluorescence (AF). Correlations between imaging modalities are indicated with vertical (white) and horizontal (green) lines. In stage 3, the fovea is darkened (color) and shows decreased reflectance (NIR) and reduced AF surrounded by hyperautofluorescence (AF imaging). Spectral-domain OCT demonstrates a characteristic optically empty space (OES), but the retinal pigment epithelium (RPE) appears intact. Note the reflective material within the OES and the thickened external limiting membrane. The extent of inner segment ellipsoid (ISe) line loss correlates with the hyporeflective area on NIR. The AF image reveals extension of the hyperautofluorescence into the region of ISe loss, although it is less intense than in the surrounding area. In stage 4, the fovea reveals mottled RPE changes (color), mottled hyporeflectivity and hyperreflectivity (NIR), and greatly reduced AF surrounded by a thin hyperautofluorescent rim (AF imaging). Spectral-domain OCT shows an OES and partial RPE disruption. The region of ISe loss corresponds to the lesions seen on color, NIR, and AF. In stage 5, the fovea is dark with a well-defined central area of RPE atrophy (color), is hyporeflective with a distinct highly reflective central area (NIR), and is hypoautofluorescent with a central region of greatly reduced AF and a surrounding hyperautofluorescent ring (AF imaging). Spectral-domain OCT evidences complete RPE disruption and loss of the OES. The region of ISe loss (solid vertical lines) correlates with the dark, hyporeflective, and hypoautofluorescent areas on color, NIR, and AF, respectively. The RPE disruption (interrupted vertical lines) corresponds to the atrophic, hyperreflective, and greatly hypoautofluorescent central areas on color, NIR, and AF, respectively. Note that the RPE is relatively spared outside of the disrupted zone.

Table 1

Clinical Findings in Study Participants

Patient/Sex/ Age, y	Sibling Pair	BCVA, R, L	SD-OCT Stage[a]	Color Fundus Photography	Near-Infrared Reflectance	AF
1/F/24	1	20/200, 20/200	1	Normal	Normal	Increased AF in superior and nasal fovea and parafovea
2/F/15		20/80, 20/80	1	Normal	Normal	Decreased macular pigment contrast
3/M/17		20/150, 20/150	2 (Intermittent ISe line disruption)	Normal	Hyporeflective fovea	Increased AF in temporal parafovea
4/F/45		20/80, 20/80	2 (Focal ISe line disruption)	Normal	Hyporeflective fovea	Reduced foveal AF; increased AF in inferior and temporal parafovea
5/M/23	1	20/160, 20/200	3	Dark fovea	Hyporeflective fovea	Reduced foveal AF surrounded by increased AF
6/M/23		20/200, 20/200	3	Dark fovea	Hyporeflective fovea	Reduced foveal AF surrounded by increased AF
7/M/25		20/200, 20/200	3	Hypopigmented foveola	Normal	Increased AF resulting in foveal stippling
8/M/34		20/100, 20/150	3	Hypopigmented foveola	Hyporeflective fovea	Reduced foveal AF
9/M/62		20/150, 20/150	3	Normal	Hyporeflective fovea	Reduced foveal AF
10/F/48		20/150, 20/150	4	Mottled RPE changes	Mixed hyporeflective and hyperreflective features	Greatly reduced foveal AF
11/M/24	2	20/100, 20/100	4	Mottled RPE changes	Mixed hyporeflective and hyperreflective features	Greatly reduced foveal AF surrounded by increased AF
12/M/35	2	20/150, 20/150	4	Mottled RPE changes	Mixed hyporeflective and hyperreflective features	Greatly reduced foveal AF surrounded by increased AF
13/F/10	3	20/150, 20/150	4	Well-defined area of RPE atrophy	Hyporeflective fovea with central hyperreflective area	Greatly reduced foveal AF surrounded by increased AF
14/M/13	3	20/150, 20/150	4	Well-defined area of RPE atrophy	Hyporeflective fovea with central hyperreflective area	Greatly reduced foveal AF surrounded by increased AF
15/F/21		20/100, 20/100	5 (Complete RPE disruption)	Well-defined area of RPE atrophy	Hyporeflective fovea with central hyperreflective area	Reduced foveal AF (greatly reduced centrally) surrounded by increased AF
16/M/52	4	20/200, 20/200	5 (Complete RPE disruption and ONL loss)	Atrophic macular lesion	Mixed hyporeflective and hyperreflective features	Absent foveal AF; increased AF around larger lesion
17/M/56	4	20/200, 20/200	5 (Coloboma-like macular lesion)	Excavation of macula down to sclera	Predominantly hyperreflective with hyporeflective features	Absent central macular AF

JAMA Ophthalmol. Author manuscript; available in PMC 2015 May 07.

Abbreviations: AF, autofluorescence; BCVA, best-corrected visual acuity; ISe, inner segment ellipsoid; L, left; ONL, outer nuclear layer; R, right; RPE, retinal pigment epithelium; SD-OCT, spectral-domain optical coherence tomography.

[a] Stage 1, intact outer retina; stage 2, ISe line disruption; stage 3, optically empty space; stage 4, optically empty space with partial RPE disruption; and stage 5, complete RPE disruption and/or loss of the ONL.

Table 2
Results of Genetic Analysis in Study Participants

Case (Pair)	Gene	Allele 1 (Mutation)	Allele 2 (Mutation)
1 (1)	*CNGB3*	c.1432C>T (p.Arg478stop)	c.1432C>T (p.Arg478stop)
2	*CNGA3*	c.829C>T (p.Arg277Cys)	c.1228C>T (p.Arg410Trp)
3	No mutations found	None	None
4	*CNGB3*	c.1056-3C>G heterozygous[a]	None
5 (1)	*CNGB3*	c.1432C>T (p.Arg478stop)	c.1432C>T (p.Arg478stop)
6	*CNGA3*	c.1391T>G (p.Leu464Arg)[b]	c.1641C>A (p.Phe547Leu)
7	*CNGA3*	c.1391T>G (p.Leu464Arg)[b]	c.1621C>T (p.Leu541Phe)[b]
8	*CNGA3*	c.1070A>G (p.Tyr357Cys)[b]	c.830G>A (p.Arg277His)
9	*CNGA3*	c.829C>T (p.Arg277Cys)	c.847C>T (p.Arg283Trp)
10	*CNGB3*	c.1006G>T (p.Glu336stop)	c.1148delC (p.Thr383IIefsX13)
11 (2)	*CNGB3*	c.1208G>A (p.Arg403Gln) heterozygous	None
12 (2)	*CNGB3* wild type	None	None
13 (3)	No mutations found	None	None
14 (3)	No mutations found	None	None
15	No mutations found	None	None
16 (4)	*CNGA3*	c.668G>A (p.Arg223Gln)[b]	c.667C>T (p.Arg223Trp)
17 (4)	*CNGA3*	c.668G>A (p.Arg223Gln)[b]	c.667C>T (p.Arg223Trp)

[a] Novel sequence variant with unknown disease relevance.

[b] Mutation was novel.